Flow of a Single Magnetic Vortex in a Submicron-Size Superconducting Al Disk Controlled by Radio-Frequency Currents

Atsushi Harada,[1] Kengo Enomoto,[1] Yamaguchi Takahide,[1] Motoi Kimata,[1] Taro Yakabe,[1] Kota Kodama,[1,2] Hidetaka Satsukawa,[1] Nobuyuki Kurita,[1] Satoshi Tsuchiya,[1] Taichi Terashima,[1] and Shinya Uji[1,2,*]

[1]*National Institute for Materials Science, Ibaraki 305-0003, Japan*

[2]*Graduate School of Pure and Applied Sciences, University of Tsukuba, Ibaraki 305-0003, Japan*

(Received 15 November 2010; published 9 August 2011)

We report the first observation of a single-vortex flow in a mesoscopic superconductor. A flow of a single vortex is successfully controlled by an rf current superimposed on a dc current, evidence of which is provided by voltage steps in current-voltage (I-V) characteristics. Irrespective of the number of vortices confined to the disk, we unambiguously observe that when a single vortex inside the disk is driven out of the disk, another vortex enters the disk similarly to two balls colliding in billiards: only one vortex passes through the Al disk at the same time in mesoscopic systems.

DOI: 10.1103/PhysRevLett.107.077002 PACS numbers: 74.78.Na, 74.25.Uv

Since the rapid development of microfabrication techniques, superconducting vortex states and their dynamics in small structures comparable to the size of Cooper pairs have attracted much attention owing to novel physical properties and their potential application as next-generation devices [1]. Several nontrivial facts have come to light through the study of mesoscopic systems despite the difficulty in measuring such small samples. In magnetic fields, the phase transitions of mesoscopic vortex states can be directly observed by micrometer Hall magnetometry [2]. Characteristic vortex configurations such as the giant vortex state (GVS) [1,3,4], the multivortex state (MVS) [5–7], and their combinations are formed, which are explained by the competition between the vortex-vortex repulsion and the confinement potential. Furthermore, sample symmetries induce unique configurations such as the coexistence of an antivortex at the center and vortices near the corners [8]. Compared with the extensive studies on static vortex states, however, there have been very few experimental reports on vortex dynamics in mesoscopic superconductors.

It is known that the collective motion of a vortex lattice in large superconducting films can be controlled by an rf current superimposed on a dc current, evidence of which is provided by voltage steps in current-voltage (I-V) characteristics, analogous to Shapiro step in weak-linked superconductors [9–11]. However, the dynamical control of a single vortex has not been achieved so far. Recently, we have reported that excess resistance much larger than the normal-state resistance emerges near the critical field in mesoscopic Al disks where a small number of vortices are confined [12]. We suggested that vortex dynamics plays a crucial role in the occurrence of excess resistance [12,13].

In this Letter, we report clear evidence of the flow control of a single vortex in a mesoscopic superconducting Al disk. We unambiguously observe that when a single vortex inside the disk is driven out of the disk, another vortex enters the disk. Irrespective of the number of vortices confined to the disk, only one vortex passes through the Al disk. Our results suggests that an entering vortex pushes out one of the vortices bound to the inside disk in a mesoscopic superconductor.

The pattern of the sample was drawn on a SiO_2 substrate by using an electron beam lithography. A 20 nm thick Al film was deposited by evaporation of high purity Al (99.999%) in vacuum, followed by a lift-off processing. Scanning electron microscope (SEM) measurements confirmed the presence of an aluminum surface with no major cracks or holes. We prepared a disk with a diameter of 0.7 μm, connecting with 0.1 μm wide Al leads, as illustrated in Fig. 1(a). The electric resistance is measured by lock-in amplifiers at the frequency of $\sim$20 Hz with the ac current $I_{ac} = 50$ nA down to $T = 0.41$ K. The magnetic field was applied perpendicular to the sample plane up to $H = 1000$ Oe. The I-V characteristics are measured by the dc techniques. All the electrical leads were shielded by low-pass filters (60 dB cutoff at 100 MHz) located near the samples. An external rf signal with a maximum incident power of 25 mW at the frequency of 240–880 MHz is transmitted by a coaxial cable capacitively coupled to the current leads. Because of the impedance mismatch with the rf transmission line, the actual rf power applied to the samples is much smaller than the incident power.

Figure 1(a) shows a contour plot of the resistance of a mesoscopic Al disk. Excess resistance is observed between the zero-resistance region and the normal state. The periodic suppression of the zero-resistance region denoted by the dotted lines is due to vorticity transitions, where the superconducting transition temperature (T_c) is rapidly reduced [1,13–15]. The vorticity L is the number of vortices confined to the sample. Figures 1(b)–1(d) show the three representative I-V characteristics. Deep inside the zero-resistance region in Fig. 1(a), the superconductivity is suddenly broken at about $I \sim 9$ μA and the normal state

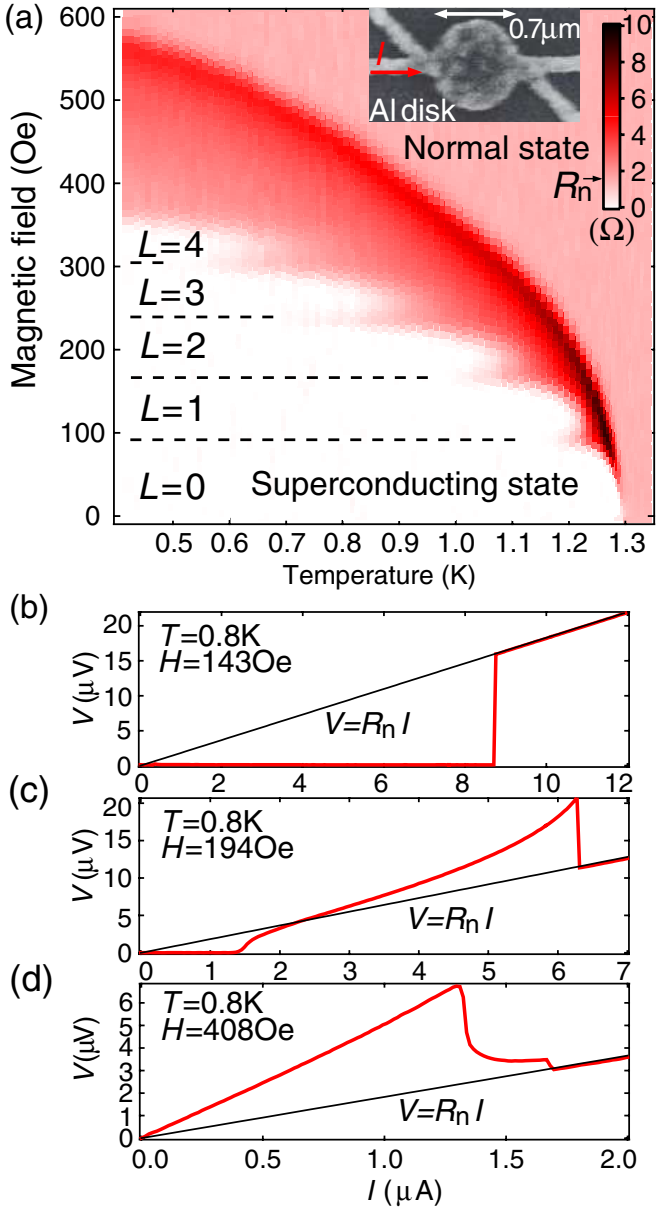

FIG. 1 (color online). (a) Contour plot of the resistance measured with a low-frequency ac current ($I_{ac} = 50$ nA) for a mesoscopic Al disk of 0.7 μm diameter. The dashed lines indicate the vorticity (L) transitions in the $R = 0$ region. The inset shows an SEM image of the sample. (b)–(d) I-V characteristics of the disk in the absence of an rf current under various magnetic fields at $T = 0.8$ K. The solid lines indicate the linear dependence $V = R_n I$, where R_n is the normal-state resistance.

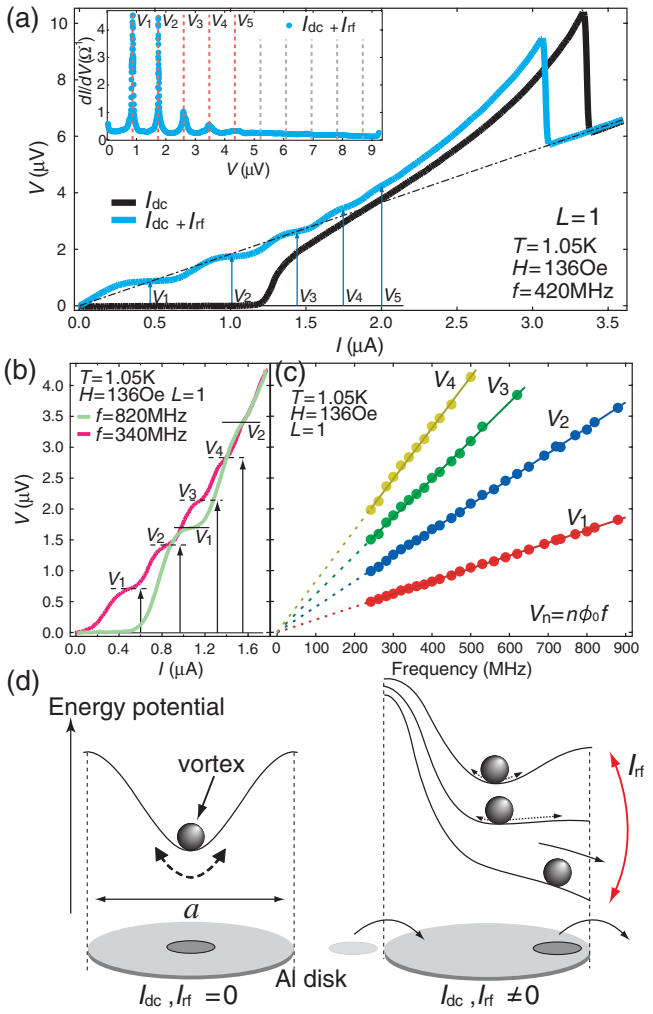

FIG. 2 (color online). (a) I-V characteristics of an Al disk with and without a superimposed rf current (I_{rf}) of $f = 420$ MHz for $L = 1$. The superimposition of I_{rf} on the dc current (I_{dc}) induces equidistant voltage steps (V_n). The inset shows dI/dV vs V with the superimposed I_{rf}. The dashed lines indicate $V_n = n\phi_0 f$ for $f = 420$ MHz. (b) I-V characteristics of the Al disk with superimposed I_{rf} of $f = 340$ and 820 MHz. (c) Frequency (f) dependence of V_n ($n = 1, 2, 3, 4$) for $L = 1$. The solid lines show $V_n = n\phi_0 f$. (d) Schematic diagram of a single vortex in a mesoscopic Al disk at I_{dc}, $I_{rf} = 0$ (left) and I_{dc}, $I_{rf} \neq 0$ (right). The number of times (n) that the vortex passes through the disk within the period $1/f$ is controlled by the rf current. The voltage steps appear when the flow rate is locked by the rf current.

is recovered, as shown in Fig. 1(b). This transition is caused by the pair-breaking effect due to the current or by the Joule heating effect at the contacts between the sample and the leads. In higher fields, characteristic broad superconducting transitions emerge, as shown in Figs. 1(c) and 1(d), where the excess resistance at a sample voltage larger than $R_n I$ is evident over a wide range of current.

At $T = 1.05$ K and $H = 136$ Oe, where a single vortex is confined to the Al disk ($L = 1$ state), a broad superconducting transition (black curve) is observed above $I \sim 1.2$ μA in the I-V characteristics, as shown in Fig. 2(a). When an rf current is superimposed on the dc current, the region of zero resistance is strongly suppressed and periodic voltage steps V_n ($n = 1, 2, 3, 4, 5$) appear up to $I \sim 2$ μA. The voltage steps are observed for $L \geq 1$ but never observed for $L = 0$. This demonstrates that voltage steps are closely related to the vortex flow. As shown in Figs. 2(b) and 2(c), the voltage steps V_n depend on the rf frequency, and have a linear frequency dependence.

Similar voltage steps in large superconducting films can be understood in terms of the interference between a vortex flow and an rf current, where a large number of vortices come into existence [9–11].

For $L = 1$, a single vortex is statically confined to the disk owing to the edge barrier [16] in the absence of an external current, as illustrated in the left figure of Fig. 2(d). A sufficiently large current drives the vortex out of the disk beyond the barrier. At that time, another vortex is driven into the disk to preserve the vorticity L because the energy levels of the $L = 0$ and $L = 2$ states are higher than that of $L = 1$ [14,15]. When a single vortex with the flux quantum ϕ_0 ($\phi_0 = h/2e$) passes through the disk, the phase difference θ of the superconducting state between the voltage contacts changes by 2π, which generates a finite voltage given by Josephson relation $\partial\theta/\partial t = 2\ \mathrm{eV}/\hbar$. This is the microscopic origin of the energy dissipation due to the vortex flow. When an rf current is superimposed, the vortex flow rate is locked by the rf frequency, causing the voltage steps, as illustrated in the right figure of Fig. 2(d) [9–11]. When the single vortex passes through the disk n times within the rf period $1/f$ ($\partial\theta/\partial t = 2\pi nf$), we obtain the voltage steps $V_n = n\phi_0 f$ ($n = 0, 1, 2, 3, \ldots$), which closely reproduces the data in Fig. 2(c) without the adjustment of any parameters. The voltage steps $V_n = n\phi_0 f$ give clear evidence of single-vortex flow in the mesoscopic Al disk. The vortex flow can be regarded as a kind of "billiards": a billiard ball (vortex) collides with another staying on a table (Al disk). The vortex flow rate (n) is controlled by the amplitude of the rf current; a vortex flow with a higher value of n becomes dominant as the rf amplitude increases.

The I-V characteristics at various rf powers (P) for $L = 1$ are shown in Fig. 3(a). As the rf power increases, the critical current ($V = 0$ region) is reduced but the values of V_n do not change. At $P = 12.4$ dBm, voltage steps above $R_n I$ are observed. The results clearly indicate that the vortex flow resistance can exceed the normal-state resistance, consistent with the previous reports [12,13]. Because of the sample inhomogeneity which cannot be detected by SEM and/or the leads-disk structure, phase slip centers (PSCs) or static superconducting-normal (S-N) boundaries may be formed between the voltage probes, especially near the contacts between the leads and disk, in the vicinity of superconducting transition. Near the PSCs and S-N boundaries, Cooper-pair or quasiparticle charge imbalance [17] is induced, which would increase the resistance as has been observed in the wire samples [18,19]. In the dark region of Fig. 1(a) adjacent to the boundary with the normal state, such Cooper-pair or quasiparticle charge imbalance would contribute to the excess resistance. It is known that the dynamical process of the PSCs synchronized with the external rf current could cause Shapiro-step-like behavior in the I-V curves [20]. However, the voltage steps are observed only for $L \geq 1$ but never observed for $L = 0$. This fact shows that such synchronization effect of the PSCs is negligibly small for our sample. Moreover, some additional background voltage due to PSCs or S-N boundaries could be added to the I-V characteristics shown in Fig. 3(a). However, such background is also quite small since the well-defined voltage steps $V_n = n\phi_0 f$ are observed.

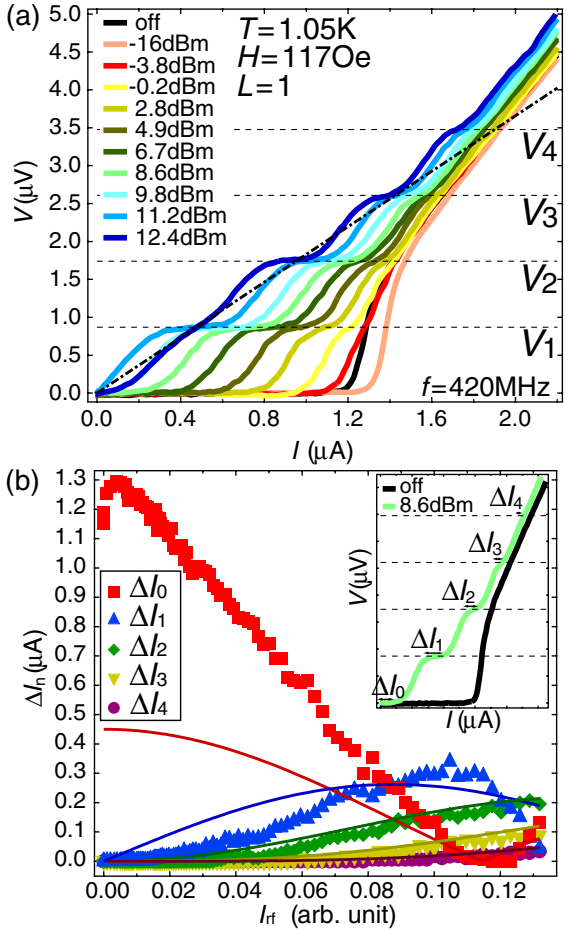

FIG. 3 (color online). (a) I-V characteristics with various rf powers (P) for $f = 420$ MHz when $L = 1$. The dashed lines and the dot-dashed line indicate the voltage steps and $V = R_n I$, respectively. (b) I_{rf} dependence of ΔI_n ($n = 0, 1, 2, 3, 4$). The values of I_{rf} are obtained from $I_{\mathrm{rf}} \propto \sqrt{P}$, and ΔI_n is determined in the voltage range of $\Delta V = \pm 0.05\ \mu$V at each voltage step (inset). The solid lines are the theoretical curves calculated using $\Delta I_n = \alpha|\mathcal{J}_n(\beta I_{\mathrm{rf}})|$, where $\alpha = 0.45\ \mu$A and $\beta = 21$.

The current width ΔI_n ($n = 0, 1, 2, 3, 4$) at each voltage step is plotted as a function of I_{rf} in Fig. 3(b). The current width can be calculated from the equation of motion for a vortex flow with a sinusoidal potential barrier [21–23]. On the assumption of a small potential barrier (high flow velocity), the width is given by $\Delta I_n = \alpha|\mathcal{J}_n(\beta I_{\mathrm{rf}})|$, where $\mathcal{J}_n$ is the Bessel function of the first kind of order n and α and β are constants depending on the critical current without I_{rf} and the dc current, respectively. The solid curves in Fig. 3(b) show the calculated results, where the

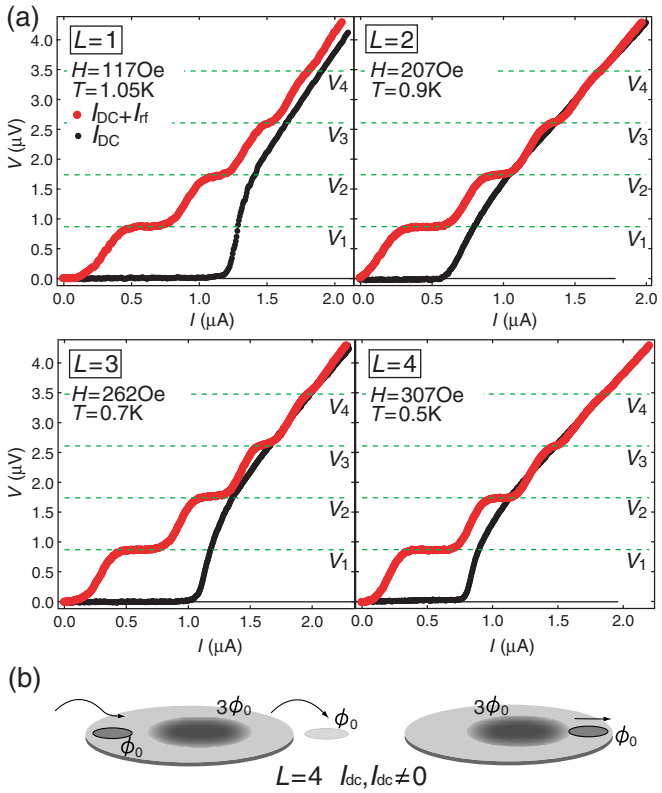

FIG. 4 (color online). (a) I-V characteristics of the Al disk with and without the superimposed $f = 420$ MHz I_{rf} for $L = 1$, 2, 3, and 4. Irrespective of the value of L in the Al disk, voltage plateaus appear at $n\phi_0 f$ (dashed lines). (b) Illustration of vortex billiards for the $L = 4$ state. The detailed configuration of the three vortices inside the disk cannot be specified.

parameters are determined by the fitting of the ΔI_2 data. Overall features are well reproduced by the calculation. The agreement with the ΔI_n data for $n = 0$, 1 is not satisfactory but we should note that the assumption of a small potential barrier is not realistic for small n. An interesting feature, a maximum of ΔI_0 for $I_{\mathrm{rf}} = 0.05$, is found, whose origin is unclear.

We measured the I-V characteristics at several different values of L, as shown in Fig. 4(a). Irrespective of the number of vortices confined to the disk ($L = 1$, 2, 3, 4), voltage plateaus appear at $n\phi_0 f$ ($n = 0, 1, 2, 3, \ldots$). The presence of the $n = 1$ step clearly shows the single-vortex flow even for $L \geq 2$. It is very likely that only one vortex can pass through the Al disk at the same time. The results for $L \geq 2$ can be also well understood in terms of vortex billiards in that an entering vortex pushes out one of the vortices bound to the inside disk, as illustrated in Fig. 4(b). Eventually, this process takes place n times within the rf period irrespective of the value of L. The detailed vortex configuration (GVS, MVS, or their combination) in the disk cannot be specified by the present measurements.

In summary, we have first managed to control the flow of a single vortex in a mesoscopic superconducting Al disk, causing the voltage steps in I-V characteristics. Irrespective of the number of vortices confined to the disk, we unambiguously observe that when a single vortex inside the disk is driven out of the disk, another vortex enters the disk similarly to two balls colliding in billiards.

We thank N. Kokubo for valuable discussions. This work was partially supported by Grant-in-Aid for Young Scientists B (No. 21740269) from the Japan Society for the Promotion of Science (JSPS) and Grant-in-Aid for Scientific Research on Innovative Areas (No. 20110004) from MEXT Japan.

*UJI.Shinya@nims.go.jp

[1] V. V. Moshchalkov *et al.*, Nature (London) **373**, 319 (1995).
[2] A. K. Geim *et al.*, Nature (London) **390**, 259 (1997).
[3] V. V. Moshchalkov, X. G. Qiu, and V. Bruyndoncx, Phys. Rev. B **55**, 11 793 (1997).
[4] V. Bruyndoncx *et al.*, Phys. Rev. B **60**, 4285 (1999).
[5] V. A. Schweigert, F. M. Peeters, and P. S. Deo, Phys. Rev. Lett. **81**, 2783 (1998).
[6] B. J. Baelus and F. M. Peeters, Phys. Rev. B **65**, 104515 (2002).
[7] A. Kanda, B. J. Baelus, F. M. Peeters, K. Kadowaki, and Y. Ootuka, Phys. Rev. Lett. **93**, 257002 (2004).
[8] L. F. Chibotaru *et al.*, Nature (London) **408**, 833 (2000).
[9] A. T. Fiory, Phys. Rev. Lett. **27**, 501 (1971).
[10] P. Martinoli *et al.*, Solid State Commun. **17**, 205 (1975).
[11] N. Kokubo, R. Besseling, V. M. Vinokur, and P. H. Kes, Phys. Rev. Lett. **88**, 247004 (2002).
[12] K. Enomoto *et al.*, Physica (Amsterdam) **29E**, 584 (2005).
[13] A. Harada *et al.*, Phys. Rev. B **81**, 174501 (2010).
[14] O. Buisson *et al.*, Phys. Lett. A **150**, 36 (1990).
[15] R. Benoist *et al.*, Z. Phys. B **103**, 377 (1997).
[16] C. P. Bean and J. D. Livingston, Phys. Rev. Lett. **12**, 14 (1964).
[17] K. Yu. Arutyunov, Phys. Rev. B **53**, 12 304 (1996).
[18] C. Strunk *et al.*, Phys. Rev. B **57**, 10 854 (1998).
[19] K. Yu. Arutyunov *et al.*, Phys. Rev. B **59**, 6487 (1999).
[20] J. D. Meyer, Appl. Phys. **2**, 303 (1973).
[21] J. R. Waldram *et al.*, Phil. Trans. R. Soc. A **268**, 265 (1970).
[22] P. Martinoli, Phys. Rev. B **17**, 1175 (1978).
[23] N. Kokubo, R. Besseling, and P. H. Kes, Phys. Rev. B **69**, 064504 (2004).